



# Analytical model of sea level elevation during a storm: Support for coastal flood risk assessment associated with cyclone passage



Natan Zambroni Maia\*, Lauro Julio Calliari, João Luiz Nicolodi

Laboratório de Oceanografia Geológica, Universidade Federal do Rio Grande (FURG), CP 474, CEP 96201–900 Rio Grande, Brazil

## ARTICLE INFO

### Article history:

Received 5 August 2015

Received in revised form

9 April 2016

Accepted 19 April 2016

Available online 3 May 2016

### Keywords:

Storm surge

Wave run-up

Wind set-up

Barometric set-up

## ABSTRACT

Sea level oscillations are a result of continuous astronomic, oceanographic, and atmospheric interactions on different time and intensity scales. Thus, the collective action of forcing factors such as tide, wind, atmospheric pressure, and wave action may lead to elevated sea levels during cyclone events over the continental shelf, abruptly impacting adjacent coasts. The objective of this study is to evaluate the potential risks of sea level rise and coastal flooding associated with the passage of cyclones in southern Brazil. An analytical model was developed based on extreme storm events from 1997 to 2008. The model identifies the impact of each forcing factor during temporary sea level rise. Through the development of a digital terrain model, it was possible to identify the areas most vulnerable to flooding by superimposing the terrain model onto calculated sea levels. During storm events, sea level elevations ranged from 2 to 5 m and show wind as the major forcing factor, followed by swells waves, astronomical tide and finally atmospheric pressure.

© 2016 Elsevier Ltd. All rights reserved.

## 1. Introduction

Sea level oscillations continuously respond to astronomical, oceanographic and atmospheric interactions, with a wide range of periodicity (Gill, 1982). Thus, all sea level records contain a complex signature spectrum that includes the tides with periods of less than 1 day to the global eustatic secular changes that occur with longer periods (Goring, 1995). In the intermediate range between 3 and 15 days, atmospheric pressure and wind variations affect sea level. This meteorological influence produces low oscillating flows in the sea level, known as storm surges, which can propagate along or towards the coastline (Truccolo et al., 2006). According to Pugh (1987), meteorological tides can be defined as the difference between the observed and astronomical tides, which may be negative or positive (“storm surge”). The storm surge is therefore responsible for the increase or decrease in sea level in relation to the astronomical tide observed at a given location. This phenomenon is positive and generally more important when the records exceed those provided by the astronomical tide, which implies seawater intrusion into places where this usually does not happen, causing major flooding (Marone and Camargo, 1994). However, when negative, the storm surge has considerable effects on port activities.

The storm surge phenomenon consists of two major components: the wind friction on the sea surface allows momentum transfer from the atmosphere to the ocean, and strong winds blowing along an oceanic track towards the mainland leads to the “pile up” of water in the coastal zone (“wind set-up”), while the low barometric pressure associated with the cyclonic rotation increases the level of the ocean (the inverted barometer effect - “barometric set-up”, Pugh, 1987; Benavente et al., 2006).

Additionally, a third factor, the increase in the wave height, also acts to increase the water level in the surf zone (“wave set-up”), allowing the waves to reach further in land than normal waves do, which transfers the surf zone towards the coast (Benavente et al., 2006). Thus, according to Marone and Camargo (1994), positive storm surges may be intensified depending on the amplitude and period of the waves that often accompany these events when they are most significant.

During high-energy conditions (storm cycles), the average level of the sea water increases by a combination of the tide, wind, wave and pressure. Thus, the beach and dunes are strongly attacked by the incident waves, which generally causes erosion. When storm waves reach the beach, they break with great intensity, and as a result, a large volume of water is released on to the beach (Van Rijn, 2009).

It is understood then that besides the rise in sea level due to the presence of a long wave on the platform (tide), there is water on the shore resulting from the wave breaking process (Marone and Camargo, 1994), where the gradient of atmospheric pressure causes the formation of winds, which in turn are responsible for

\* Corresponding author.

E-mail addresses: [natanzambroni@yahoo.com.br](mailto:natanzambroni@yahoo.com.br) (N.Z. Maia), [lcalliari@log.furg.br](mailto:lcalliari@log.furg.br) (L.J. Calliari), [joaluiznicolodi@gmail.com](mailto:joaluiznicolodi@gmail.com) (J.L. Nicolodi).

generating waves and increasing the sea level. When the air pressure gradient is very intense, there is the possibility that tropical cyclones will form, leading to the generation of tall waves that propagate as swells over long distances to the shore. Water stacking by these waves associated with astronomical spring tides accentuates the erosive power active on the coast to cause super elevation above the tidal prism (Parise, 2007).

The combination of positive meteorological tides with wave set-up can result in extreme values of wave run-up (maximum vertical excursion of swash on the beach face), which can result in the overtopping of dunes as well as structures of coastal protection, especially when these storms coincide with astronomical spring tides. Thus, flooding and erosion can occur in areas where they do not normally occur (Benavente et al., 2006). According to Ferreira et al. (2006), the storms associated with storm surges are the most important factor controlling shoreline movement in the short term.

Thus, the effects of storm surges on the coast may result in many losses for coastal communities, such as by depositing fluid mud on the beach (Calliari and Faria, 2003), the loss of land, the destruction of property and natural habitats, estate depreciation and tourism, the reduction in tax collection and the loss of lives (Teixeira, 2007). However, the distribution of the effects of a storm on a coast depends on many variables, such as subaqueous morphology, refraction and diffraction patterns of waves, sediment budgets, morphodynamic behavior of beaches, dune development and also human interventions and coast line uses (Balsillie, 1986; Lawrence, 1994 *apud* Benavente et al., 2002; Toldo et al., 2010).

The potential consequences of these storm simply the need for tools that recognize vulnerable areas at risk of flooding. This factor has been modeled, and the resulting information forms the basis for mappings of coastal risk (Benavente et al., 2006), as noted in Van Cooten et al. (2011), that coupled hydrodynamic, hydrological and atmospheric models aiming to measure sea level rises during

storms and hurricanes in the American coast. Also on the American continent, a great effort has been made in order to study the effect of storm surges on the coast through the Economic Commission for Latin America (CEPAL, 2011), under the project Effects of Climate Change in Latin America and Caribbean coasts. This project uses wave and tidal reanalysis data from the SMC-Brazil model developed by the Hydraulic Institute of Cantabria, Spain. Also on the Brazilian coast, several studies have been developed on this theme, as in Machado and Calliari (2016) that studied the cyclone lifecycle to identify the trajectory of them aiming to predict potential impacts on the southern Brazilian coast. For this same stretch of the coast of Brazil, Guimarães et al., (2014, 2015) combined many different wave models, Wave Watch III, SWAN and SWASH to provided the information on risk conditions during storm events, by simulating the highly dynamic zones during extreme hydrodynamic events over natural and urban structures.

In coastal areas that include an urban settlement, it is prudent to take precautions against sudden and frequent sea level rises that are potentially dangerous (Ferreira et al., 2006). The consequent retreat of coastal erosion from storms is one of the most important phenomena, and it needs to be precisely quantified to facilitate effective management strategies for coastal areas (Callaghan et al., 2009).

In this context, the present study aims to assess the risks related to coastal flooding during the passage of cyclones in Hermenegildo Beach in Brazilian southern coast (Fig. 1). For this an analytical model was developed to calculate the sea level rises using wave, wind, pressure and tide data, and in additional, was also developed a Digital Terrain Model (DTM) with the topography of the area in question. Thus, identifying the contribution of each forcing in elevations and calculating the total lift on sea level quota, with overlapping of the DTM was possible to identify the most vulnerable areas to flooding during storms.

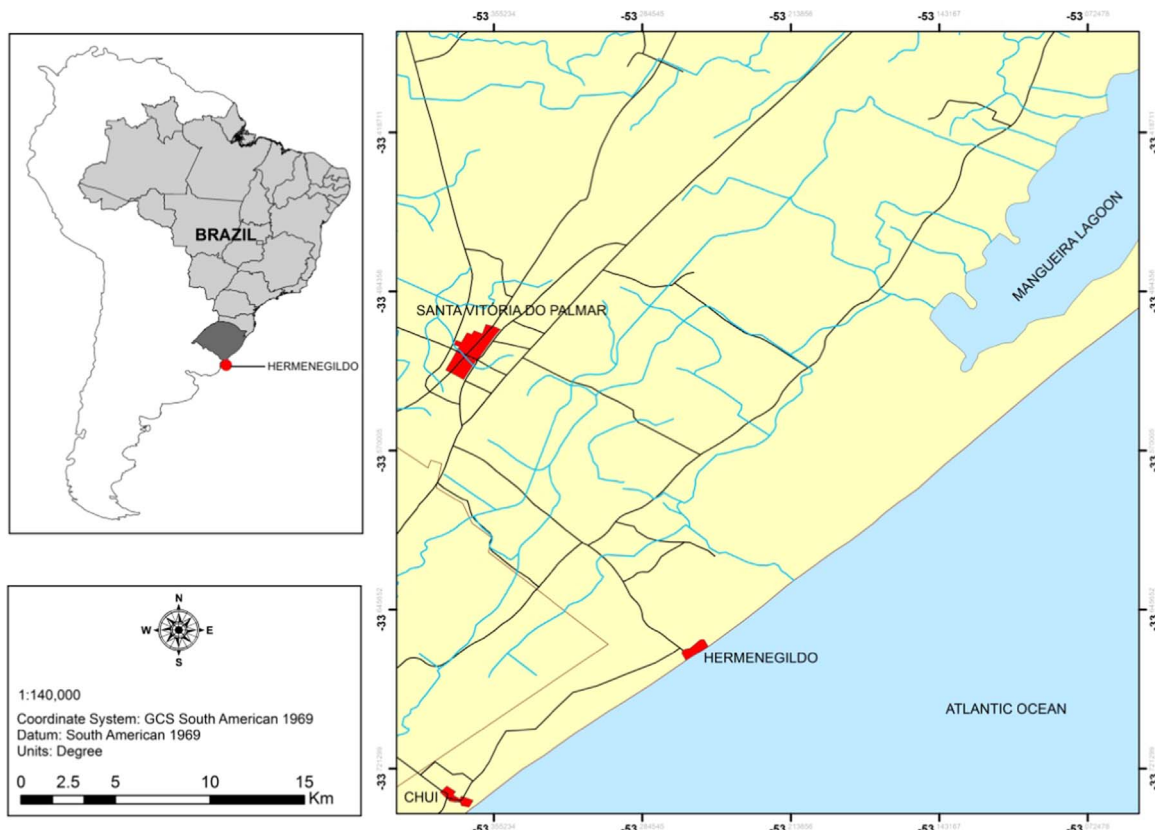


Fig. 1. Hermenegildo Beach, southern coast of Brazil.

## 2. Methodology

The methodological sequence for the development of this work followed the following chronology: gathering and processing data related to the waves, wind, pressure and astronomical tide; development and validation of an analytical model to calculate sea level elevations; implementation of the analytical model to calculate sea levels for the selected events; preparation of a digital terrain model; and, finally, preparation of the illustrations related to the calculated flood levels from 1997 to 2008 in the region where it was tested.

### 2.1. Data

#### 2.1.1. Waves

Wave data were obtained from the outputs of the model Wave Watch III NCEP/NOAA (version 2.22), available at <ftp://polar.ncep.noaa.gov/pub/history/waves>. Significant wave height and wave period were considered with a temporal resolution of 3 h. The model has a spatial resolution of  $1^\circ \times 1.25^\circ$ , with the point defined by the coordinates  $34^\circ\text{S}$  and  $52.5^\circ\text{W}$  used to obtain the data.

This point was chosen because, according to the output of the model, it is close to Hermenegildo Beach over the continental shelf and is situated approximately 80 km from the coast. The equations that govern the Wave Watch III model include wave refraction due to temporal and spatial variations of the average water depth and currents. The parameterization of physical processes includes the action of wind, nonlinear interactions, dissipation and friction with the bottom. WW3 solve the conservation equation of spectral energy density in terms of the number and wave direction as functions that vary slowly in space and time. This equation implicitly admits that the spatial and temporal scales of the waves themselves are much smaller than the corresponding variation ranges of the spectrum and the depths and currents. WW3 determines the directional spectrum evolution of field waves, which shows how this sea surface energy is distributed in terms of frequency and direction of components, being height, period and direction of waves (Tolman, 1997, 2002).

#### 2.1.2. Wind and pressure

Data on wind and atmospheric pressure came from the Reanalysis Project R-1NCEP/NCAR (National Centers for Environmental Prediction) database, which is available at <http://www.esrl.noaa.gov/psd/data/gridded/data.ncep.reanalysis.html>. Thus, it was possible to monitor the weather conditions in the study area during the passage of cyclones. The reanalysis data have a temporal resolution of 6 h and spatial resolution of  $2.5^\circ \times 2.5^\circ$ .

The NCEP/NCAR Reanalysis Project is a joint project between the National Centers for Environmental Prediction (NCEP) and the National Center for Atmospheric Research (NCAR). Reanalysis is a scientific method for developing a comprehensive record of how weather and climate are changing over time. In it, observations and a numerical model that simulates one or more aspects of the Earth system are combined objectively to generate a synthesized estimate of the state of the system. Reanalysis products are used extensively in climate research and services, including for monitoring and comparing current climate conditions with those of the past, identifying the causes of climate variations and change, and preparing climate predictions. A reanalysis typically extends over several decades or longer, and covers the entire globe from the Earth's surface. The goal of this joint effort is to produce new atmospheric analyses using historical data (1948 onwards) and as well to produce analyses of the current atmospheric. Reanalysis datasets are created by assimilating climate observations using the same climate model throughout the entire reanalysis period in order to reduce the effects of modeling changes on climate

statistics. Observations are from many different sources including ships, satellites, ground stations, RAOBS, and radar. The dataset is kept current using near real-time observations (Available at <http://www.cpc.ncep.noaa.gov/products/wesley/reanalysis.html#intro>; <http://www.esrl.noaa.gov/psd/data/gridded/reanalysis/>).

For this study, the data at the point defined by the coordinates  $32.5^\circ\text{S}$  and  $52.5^\circ\text{W}$  were used, and with respect to the wave data, this point was chosen based on the output of the template as being the closest to Hermenegildo Beach over the continental shelf. To calculate the resulting wind speed, we used the zonal (u) and meridional (v) components at a height of 10 m (Bowden, 1983), and for the atmospheric pressure, the respective values at the average sea level. According to Oliveira et al. (2007), the Reanalysis data are quite useful and satisfactory for cases in which the lack of atmospheric data is substantial.

For visualization and analysis of wind and pressure data, as well as waves, the Panoply<sup>®</sup> program (NASA/GISS) was used.

#### 2.1.3. Astronomical tide

Astronomical tide data are from the Directorate of Hydrography and Navigation (DHN) from the Brazil Navy and are available at [www.mar.mil.br/dhn/chm](http://www.mar.mil.br/dhn/chm). DHN forecast are generated from harmonic components obtained from observations made by various institutions distributed along the Brazilian coast.

In the absence of specific data for Hermenegildo Beach, it was decided to use the tide predictions for harmonic analysis for the coast adjacent to Rio Grande city, approximately 200 km from the study area. However, the two regions experience the same tidal pattern. For each event, to characterize the worst elevation scenario, the highest elevation value of the astronomical tide during the passage of cyclones along the coast was selected.

## 2.2. Methods

### 2.2.1. Development of the analytical model

An analytical model (Equation 1) was developed for sea level rise calculation during storms induced by the passage of a cyclone. The water surface elevation was calculated by taking into account each of the contributing factors described in this equation and calculates the most extreme values of sea level rise during storm events.

**2.2.1.1. Level rise induced by wind (wind set-up).** In the simplified model used in this article, it is normally a fundamental hypothesis that the wind-induced rise in the landmark is dominated by local forcing. According to this hypothesis, level variations due to remote effects that propagate along the coast in the form of platform waves are excluded.

To calculate the elevation in the wind-induced level, we used the equation proposed by Csanady (1982) for winds parallel to the shore (Equation 2).

The average of platform depth ( $H=100$  m) of Equation 4 was determined by parametric analysis, where different values have been tested without significant variations in the results. In this way it estimated the average value thereof.

The events analyzed were initially selected based on wind behavior, requiring cyclones to be located over the continental shelf and requiring the wind to flow parallel to the coast from the SW. The wind speed value entered into the equation was the average speed for the duration of the event, which was also determined from the displacement of the cyclone.

**2.2.1.2. Level rise induced by wave (wave run-up).** The increase in the wave run-up on the coast caused by increased wave height during the storms was calculated by Equation 8 proposed by Battjes (1971), which evaluates the maximum vertical wave tour

on the beach face.

Equation 8 was also used by Ferreira et al., (2006) and Freitas et al., (2010) to measure and calculate the over wash flood levels in Ancão Peninsula (Portugal) and Itapocorói (Brazil), respectively. For the wave height value entered into the equation, the average of significant heights during the duration of the event was calculated and used along with the wave period.

**2.2.1.3. Level rise induced by atmospheric pressure (barometric setup).** The sea level rise induced by atmospheric pressure was calculated from the Inverse Barometer Effect (Equation 10). According to Benavente et al. (2006), because low pressure persists for a sufficient time interval, the water level increases in a proportion of 1 cm for each millibar decrease (or 1 hPa) at atmospheric pressure at the sea surface. The Effect of Inverse Barometer describes an isostatic sea level response to the balance applied by the pressure gradient (Truccolo et al., 2006). This response was calculated, and the values for the pressure drop induced by the cyclone passage were used. Benavente et al. (2000) also used this principle to identify flooding areas along the Valdelagrana spit on the Spanish coast.

### 2.2.2. Development of the Digital Terrain Model (DTM)

For the DTM development, was used a kinematic GPS, which according to Morton et al. (1993) provides for obtaining data quickly and accurately along coastal segments. According to Morton and Speed (1998) and Pajak and Leatherman (2002), GPS with shoreline mappings are more accurate than withdrawals made by Photointerpretation, since they allow a better spatial sampling throughout the area to be mapped.

Data acquisition was performed using geodetic GPS (RTK) with planimetric accuracy of 0.005 m and altimetric of 0.02 m with cutting angle for signal receiving of 15°, as well as altimetry data referenced to the GRS-80 ellipsoid and operated with C/A code (1023 MHz) and carriers L1 (1575.42 MHz) and L2 (1227.60 MHz). Data collection was performed using the Stop and Go method and for preparing the DTM, 10,000 points were used.

**Table 1**  
Data used for analytical model validation. The values in bold are the level rises calculated by the analytical model for comparison with the measures in the field by Parise et al. (2009).

Occurrence period Parise et al. (2009)	Start of the event (day, time)	Event end (day, time)	Event Duration (hours)	Wind speed (m/s)	Cd	Wave height (m)	Wave period (s)	$\Delta P$ (hPa)	Calculated elevation (m)	Elevation Parise et al. (2009) (m)
06/17–21/06	15, 18 h	16, 18 h	24	5.61	1	2.4	8.05	8	<b>0.51</b>	<b>0.48</b>
06/21–29/06	26,12 h	27,0 h	18	13.3	1.5	4.24	8.58	28	<b>1.4</b>	<b>1.26</b>
07/07–11/06	9,6 h	9,6 h	6	15	1.6	1.1	5.8	25	<b>0.7</b>	<b>0.81</b>
07/25/06 –08/03/06	29, 0 h	30,12 h	42	12.3	1.4	4.46	10.06	17	<b>1.96</b>	<b>1.81</b>
08/19–25/06	20, 6 h	21, 12 h	36	11.9	1.4	3.8	8.84	16	<b>1.68</b>	<b>1.84</b>
09/01–08/06	2, 18 h	4, 12 h	48	14	1.45	3.94	9	24	<b>2.7</b>	<b>1.82</b>
09/22–26/06	23,6 h	24,6 h	30	11.3	1.4	2.5	6.43	18	<b>1.19</b>	<b>0.92</b>
09/26–29/06	28, 0 h	28, 12 h	18	8.6	1.2	2	7.4	8	<b>0.58</b>	<b>0.49</b>
10/04–13/06	5, 12 h	5, 18 h	12	12	1.4	2	6.7	10	<b>0.68</b>	<b>0.12</b>
11/02–13/06	6, 12 h	8, 18 h	60	10.2	1.3	3.5	9.1	27	<b>1.85</b>	<b>0.73</b>
11/24/06–12/16/06	4, 0 h	4, 6 h	12	6.8	1.2	1.4	6.22	11	<b>0.4</b>	<b>0.44</b>
02/04–9/07	7, 0 h	7, 6 h	12	10.4	1.4	1.4	7.6	15	<b>0.64</b>	<b>0.93</b>
02/14–24/07	18, 0 h	18, 12 h	18	11.1	1.4	2.14	5.6	19	<b>0.84</b>	<b>0.89</b>
03/31/07–04/14/07	8, 6 h	9, 0 h	24	10.8	1.4	2.35	6.6	14	<b>0.95</b>	<b>0.92</b>
04/25–29/07	26, 6 h	27, 18 h	42	8.7	1.2	2.8	8.7	13	<b>1.1</b>	<b>1.45</b>
05/06–11/07	6, 18 h	7, 6 h	18	10.4	1.4	2.3	6.12	18	<b>0.8</b>	<b>0.62</b>
05/22–27/07	23, 6 h	24, 6 h	30	11.2	1.4	3.3	7.74	18	<b>1.29</b>	<b>1.07</b>
05/27–31/07	29, 6 h	30, 0 h	24	10.1	1.4	3.8	9.73	6	<b>1.0</b>	<b>1.06</b>
05/31/07–06/07/07	3, 6 h	4, 6 h	30	12.1	1.4	3.92	9.67	19	<b>1.55</b>	<b>1.14</b>
06/07–20/07	15, 12 h	16, 0 h	18	15.2	1.6	2	6.3	17	<b>1.33</b>	<b>0.74</b>
06/20–28/07	27, 0 h	27, 18 h	24	6.3	1.2	1.16	10.01	19	<b>0.63</b>	<b>0.89</b>
06/28/07–07/05/07	30, 0 h	1, 18 h	48	7.53	1.2	2	8.63	21	<b>1.0</b>	<b>1.94</b>
07/05–17/07	10, 12 h	11, 0 h	18	11.3	1.4	2.6	7.9	21	<b>1.0</b>	<b>1.02</b>

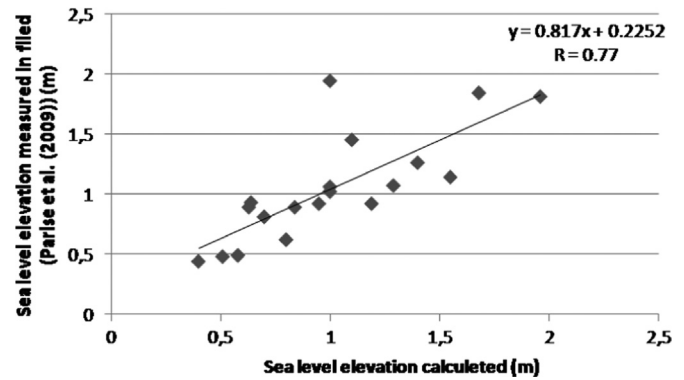


**Fig. 2.** Linear correlation between the rise in sea level values measured in the field (Parise et al., 2009) and those calculated by the analytical model.

### 2.2.3. Development of flood level illustrations

The results obtained by Equation 1 provide the values of sea level rise during a storm took place on the coast and, when compared with the elevations of the Digital Terrain Model, indicate areas of potential coastal flooding. Benavente et al. (2006) and Freitas et al. (2010) obtained satisfactory results in identifying areas vulnerable to flooding by overlapping sea level lifting quotas with their DTMs.

## 3. Results and discussion

### 3.1. Validation of the analytical model

To validate the analytical model we compared modeled sea-level rise with field measurements by Parise et al. (2009) on Cassino Beach (RS) during 2006 and 2007. These authors monitored 23 events and measured meteorological tides using topographic profiles and video monitoring. To assess the accuracy of the analytical model, we compared the values obtained by the model to those measured in the field by Parise et al. (2009) (Table 1), and

**Table 2**

Sea level elevation values calculated by the analytical model for Hermenegildo Beach during the 16 selected extreme events between 1997 and 2008.

Event number	Ocurrence period Melo et al. (2010)	Start of the event (day, time)	Event end (day, time)	Event Duration (hours)	Wind speed (m/s)	Cd	Wave height (m)	Wave period (s)	$\Delta P$ (hPa)	Astronomical tide (m)	Level elevation (m)
1	04/05/1997	4, 12 h	6, 6 h	48	10.4	1.4	3.6	11.0	14.0	0.5	<b>2.8</b>
2	05/23/1997	24, 18 h	26, 6 h	42	6.1	1.15	2.5	11.0	19.0	0.6	<b>2.0</b>
3	03/25/1998	24, 12 h	26, 12 h	54	10.5	1.4	3.0	8.1	15.0	0.4	<b>2.5</b>
4	04/18/1999	15, 12 h	19, 12 h	102	7.75	1.2	3.26	8.04	17.0	0.7	<b>2.7</b>
5	05/20/1999	18, 18 h	21, 6 h	66	9.14	1.3	3.3	8.46	12.3	0.5	<b>2.5</b>
6	05/31/1999	29, 12 h	31, 0 h	42	13.8	1.45	3.8	7.9	18.0	0.6	<b>3.3</b>
7	04/18/2000	20, 0 h	21, 18 h	48	8.6	1.2	3.2	8.7	16.5	0.5	<b>2.2</b>
8	02/02/2002	1, 6 h	2, 12 h	36	11.9	1.4	3.6	8.6	13.0	0.1	<b>2.2</b>
9	09/01/2002	31, 12 h	2, 12 h	54	12.3	1.4	4.5	11.9	18.5	0.4	<b>3.6</b>
10	05/25/2003	23, 0 h	25, 12 h	66	14.9	1.6	3.6	8.4	23.3	0.5	<b>5.0</b>
11	05/26/2004	26, 6 h	28, 0 h	48	12.7	1.4	3.8	8.9	32.0	0.6	<b>3.4</b>
12	06/27/2006	26, 6 h	27, 18 h	42	10.6	1.4	4.2	9.1	22.0	0.3	<b>2.5</b>
13	07/29/2006	28, 18 h	31, 6 h	66	11.6	1.4	4.13	9.94	14.0	-0.1	<b>2.9</b>
14	09/04/2006	2, 12 h	4, 18 h	60	13.0	1.5	3.95	9.0	28.0	0.4	<b>3.8</b>
15	08/20/2007	20, 0 h	21, 6 h	36	11.3	1.4	2.7	7.2	18.0	0.2	<b>2.0</b>
16	05/25/2008	24, 6 h	25, 18 h	42	13.2	1.5	4.0	8.9	14.0	0.6	<b>3.3</b>

calculated their correlation afterwards (Fig. 2). A positive correlation coefficient (R) was found with the value of 0.77, which is considered statistically high. However, taking into account all of the simplifications assumed for the preparation of the analytical model as well as the potential inaccuracies in the amounts recorded by Parise et al. (2009), the correlation between the data can be considered very satisfactory. The Equation 11 describes the relationship between the data. Therefore, the correlation was calculated excluding the event in which this behavior was observed, as well as the event where the meteorological tide recorded by Parise et al. (2009) presented an inconsistent value much lower than expected based on the pressure, wind and wave characteristics. Thus, this correlation excludes events recorded for the periods from 09/01/06 to 09/08/06, 10/08/06 to 10/13/06, 11/02/06 to 11/13/06 and 06/07/07 to 06/20/07.

### 3.2. Analytical model implementation

For the analytical model implementation, the most extreme events between 1997 and 2008 on the Rio Grande do Sul coast identified by Melo et al. (2010) were selected. Through numerical modeling, the authors identified the events with the highest wave heights between the years 1979 and 2008. In this study, event selection started in 1997 because the Wave Watch III wave data started that year. For Hermenegildo Beach, sea level elevation

values were then calculated using the analytical model for 16 events induced by the passage of cyclones included in this period. The sea level elevation values and their respective atmospheric and hydrodynamic characteristics are shown in Table 2.

The analytical model is very sensitive to wind conditions, allowing it to respond directly to speed increases and the time duration of the event. Thus, the final values calculated for sea level elevations at high and long durations of wind speeds can be over-estimated, since Equation 2 assumes a constant depth throughout the fluid flow to the coast and does not consider the friction with the bottom of the water, making it an inviscid solution. Thus, according to Csanady (1982), while there is wind present the water level rises linearly with time due to water stacking on shore. However, the simulations in this work can support and guide urban planning in the study area, even if the model at certain times may over-estimate the elevation of sea level on the passage of cyclones, since it is preferable to produce extreme scenarios that results under-estimated and optimistic for this type of event. Thus, as described by Van Cooten et al. (2011) with the IC-FLOW Project, this work can be used as a planning tool by coastal managers to simulate the effect of historical and/or hypothetical storms on a community, thus creating an opportunity to enhance resiliency through science-based community planning and emergency response.

**Table 3**

Contributions from each forcing factor making up the overall rise in calculated sea levels.

Event number	Ocurrence period	Wind elevation (m)	Wave elevation (m)	Pressure elevation (m)	Astronomical tide elevation (m)	Total level elevation (m)
1	04/05/1997	1.02	1.18	0.14	0.5	<b>2.8</b>
2	05/23/1997	0.25	0.99	0.19	0.6	<b>2.0</b>
3	03/25/1998	1.17	0.78	0.15	0.4	<b>2.5</b>
4	04/18/1999	1.0	0.82	0.17	0.7	<b>2.7</b>
5	05/20/1999	1.0	0.87	0.12	0.5	<b>2.5</b>
6	05/31/1999	1.63	0.87	0.18	0.6	<b>3.3</b>
7	04/18/2000	0.6	0.88	0.16	0.5	<b>2.2</b>
8	02/02/2002	1.0	0.93	0.13	0.1	<b>2.2</b>
9	09/01/2002	1.6	1.4	0.19	0.4	<b>3.6</b>
10	05/25/2003	3.3	0.9	0.23	0.5	<b>5.0</b>
11	05/26/2004	1.5	1.0	0.32	0.6	<b>3.4</b>
12	06/27/2006	0.9	1.1	0.22	0.3	<b>2.5</b>
13	07/29/2006	1.7	1.4	0.14	(-)0.1	<b>2.9</b>
14	09/04/2006	2.1	1.0	0.3	0.4	<b>3.8</b>
15	08/20/2007	0.9	0.7	0.2	0.2	<b>2.0</b>
16	05/25/2008	1.5	1.0	0.14	0.6	<b>3.3</b>

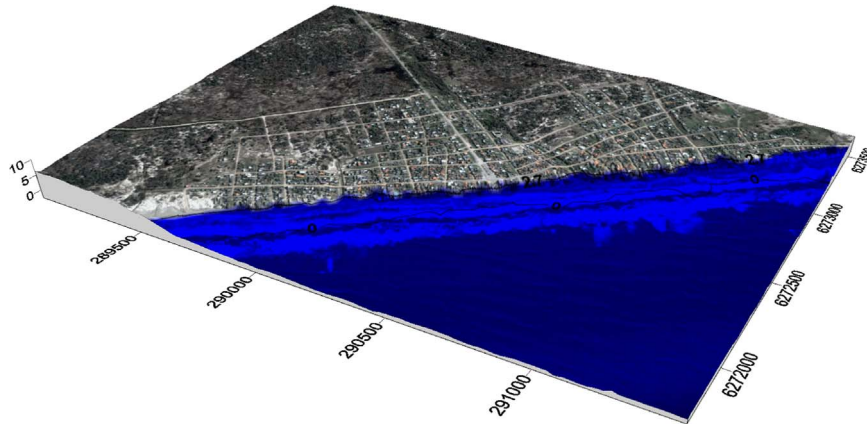


Fig. 3. Sea level elevation in 2.7 m superimposed on DTM.

### 3.3. Forcing contributions to sea level rise during the passage of cyclones

According to Benavente et al. (2006), the influence of variables that affect sea level rise during a “storm surge” depends on the intensity of storms generated by the passage of frontal systems.

Therefore, for the analysis of Table 2, it can be seen that the events presented different hydrodynamic and atmospheric behaviors, which in turn generate different values for the sea level elevation. In this sense, the values of sea level rise oscillated between 2 and 5 m during cyclone passage. These extreme values were directly related to the wind behavior, where the lowest value of sea level

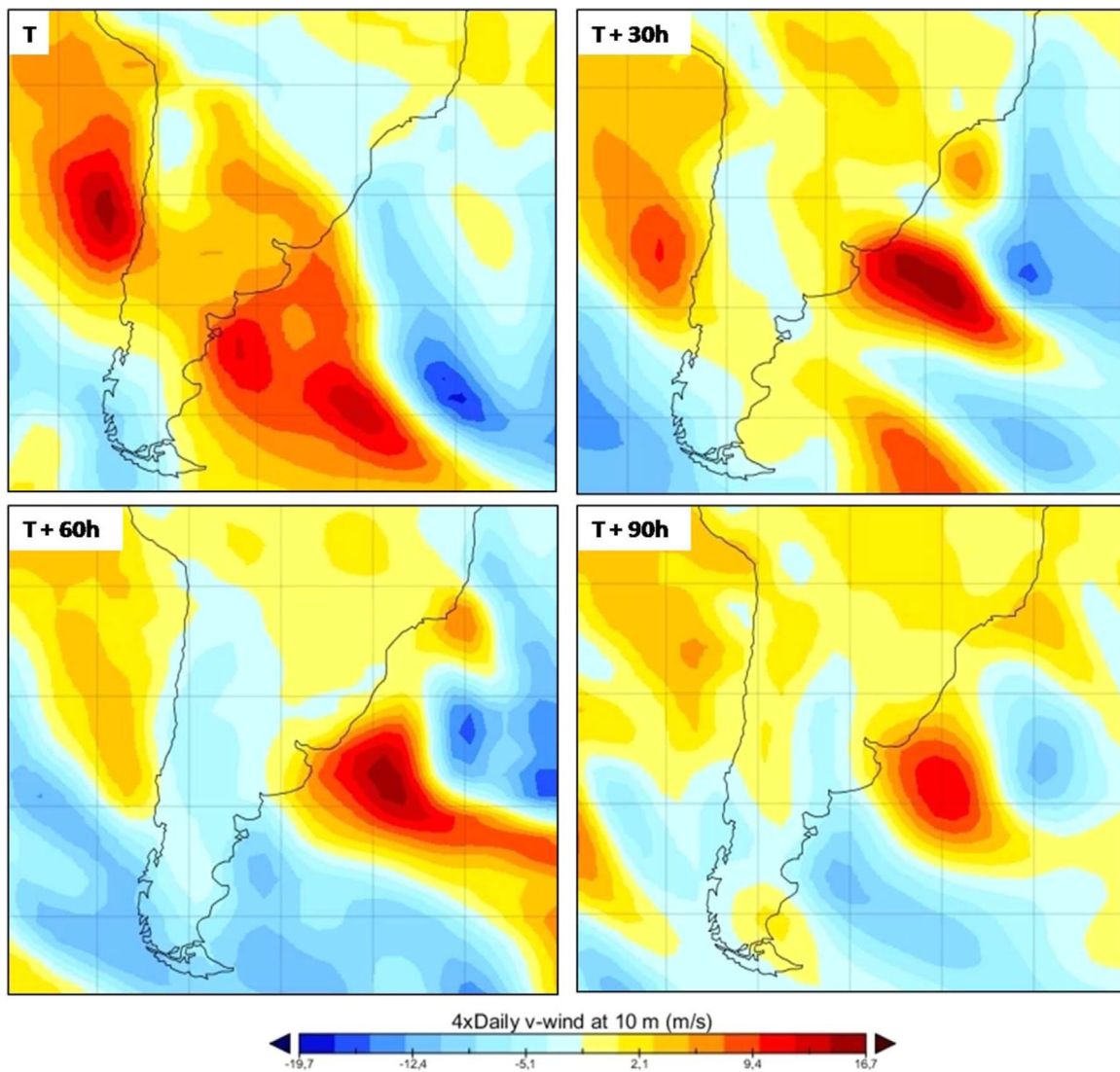


Fig. 4. Event 4. Cyclone parked in front of the studied area during 4 days.



Fig. 5. House destruction during the April 1999 event.

rise, 2 m, was recorded at a lower wind speed, 6.1 m/s. Similarly, the highest elevation level, 5 m, was recorded at the highest wind speed, 14.9 m/s. In general, referring to the contribution of each forcing factor in the elevation levels shown in Table 3, the wind has a greater contribution than the other factors to sea level rise. On average, the wind was responsible for inducing 43% of sea level rise, followed by waves at 35%, astronomical tides at 15% and finally the pressure at 7%. In studies conducted in southwestern Spain, Benavente et al. (2000) credited the wind with 60% of the sea level rise during the occurrence of a storm-induced cyclone, while the waves were credited with 30% of the rise.

Table 3 shows the contribution of each forcing factor that makes up the overall rise in sea level during the implementation of the analytical model, with the wind as the major agent responsible for the induction of positive oscillations of sea level during the passage of cyclones.

For all 16 events analyzed, the wind came from the SW, which due to the NE-SW orientation of the Rio Grande do Sul coast, produces water stacking due to the Coriolis effect. This behavior was also observed by Saraiva et al. (2003) and Parise (2007), and these authors related elevations in sea level during the passage of cyclones with a SW wind in 85% and 70% of cases, respectively. Studying the occurrence of storm surges in southern Brazil, Trucolo et al. (2006) and Xavier (2003) also found the wind parallel to the coast to be the main water truck agent on the coast. According to the authors, the main forcing factors that promote positive and negative fluctuations in sea level are the longitudinal / meridional

components to wind stress on the coast, with atmospheric pressure playing a secondary role.

### 3.4. Sea level elevation

Table 2 provides sea level elevation values calculated for the selected events. Comparing and superimposing these values on to elevations of the Digital Terrain Model indicate areas of potential coastal flooding. It is noteworthy that the flood levels are related to elevations of the land base and do not take into account the interactions between water and structures on the ground. However, these models can be used to evaluate worst case scenarios for lifting levels during storms (Ferreira et al., 2006). In this sense, as adopted by Tagliani et al. (2010), in a scenario of flooding, a major factor to consider is the elevation of the terrain where the lower altitudes are more vulnerable to rises in sea level, water cannot reach attainable sites or in the larger spring tide.

For the 16 events analyzed, we calculated 11 distinct values of elevation level resulting from the passage of cyclones, oscillating between 2 and 5 m. To identify the flooding vulnerability, the calculated results were superimposed on to the Digital Terrain Model of Hermenegildo Beach. Two of the specific cases will be discussed below. In Maia (2011), you can see in detail all sea level rising situations identified in Table 2.

#### 3.4.1. Sea level elevation at 2.7 m

The elevation level at 2.7 m was calculated for the event that occurred on 04/18/1999 (Event 4), which is illustrated in Fig. 3. In this event, the illustration indicates a greater intrusion of the sea on to the beach, so that virtually all buildings located on the second line of houses parallel to the beach are affected by sea water, including those located at the northern and southern urbanized limits of Hermenegildo Beach. However, at the southern end of the same stretch in front of the preserved dunes, the water still remains on the face of the beach. This event presented two important features, a large contribution from the astronomical tide, 26%, and a very high time of event duration, with the cyclone staying on the platform for 102 h (Fig. 4), the highest among all cases analyzed. According to Machado et al. (2010), the meteorological scenario of this event was highly unusual because the cyclone path on the platform developed in a circular manner, without major zonal and meridional movements, and then practically remained parked opposite the Rio Grande do Sul coast.

Given its impact on the coast, several author shave studied the

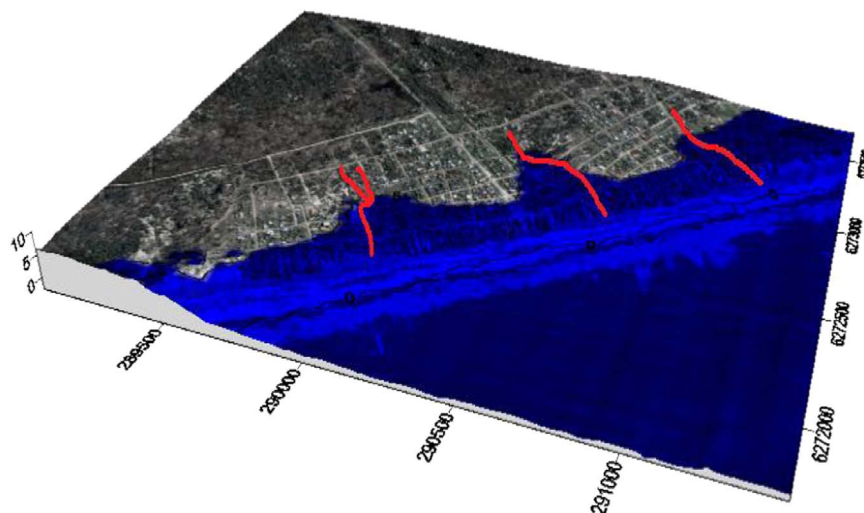


Fig. 6. Sea level elevation in 5 m superimposed on DTM. The inlets are indicated in red.(For interpretation of the references to color in this figure legend, the reader is referred to the web version of this article.)

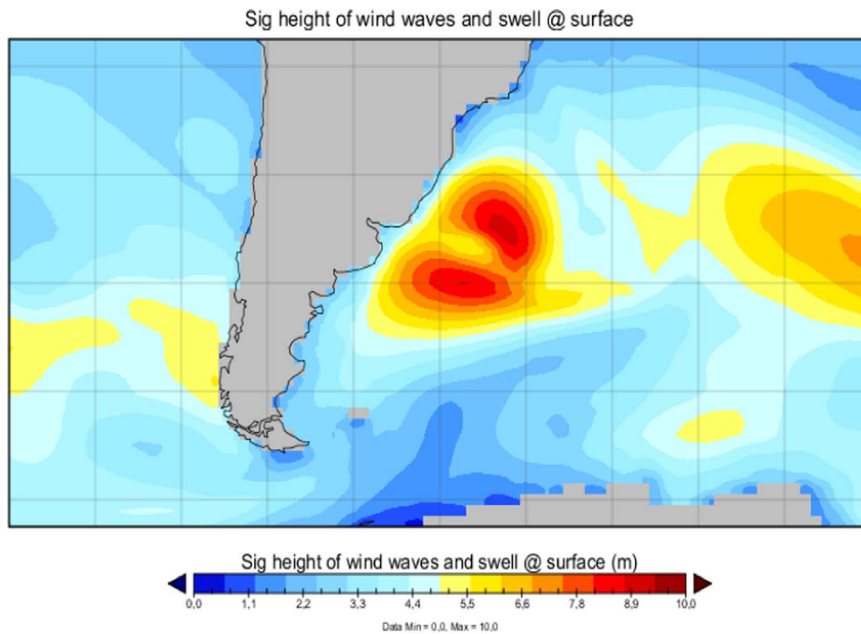


Fig. 7. Significant wave height during event 10.

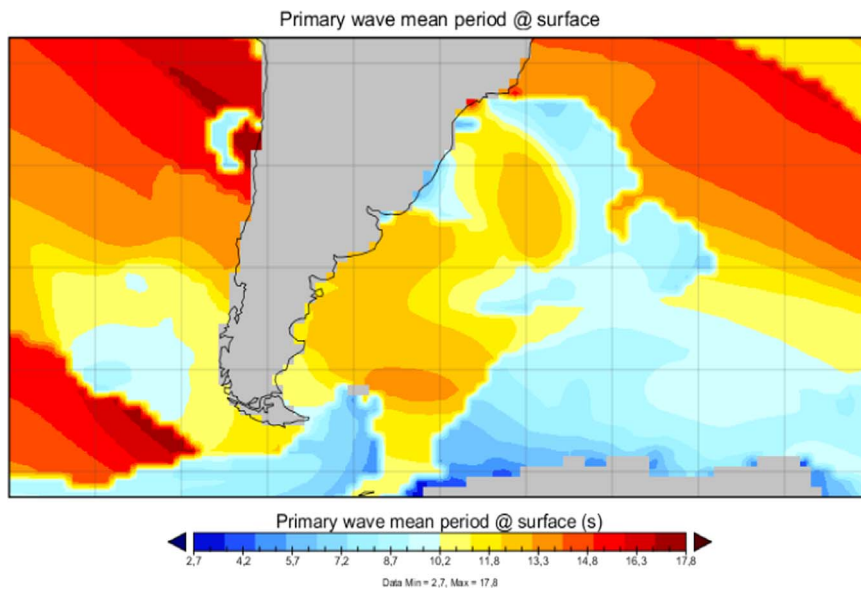


Fig. 8. Wave period during event 10.

event that occurred in April 1999. According to [Esteves et al. \(2000\)](#), during this event on the Rio Grande do Sul shore, winds up to 115 km/h were recorded, and waves up to 8 m were measured by wave rider at a 15 m depth. Using modeling of wave propagation, [Goulart \(2010\)](#) found waves up to 9.2 m in the state. According to [Esteves et al. \(1999\)](#) as well as [Santos and Esteves \(2001\)](#), these high-energy conditions resulted in critical erosion on Hermenegildo Beach, causing the total destruction of 20% of sea side houses and countless losses to structure, as illustrated in [Fig. 5](#). According to [Tozzi and e Calliari \(2000\)](#) the April 1999 storm was a typical example of high-energy events that threaten the Hermenegildo resort at least once a year.

#### 3.4.2. Sea level elevation at 5.0 m

The increase in level of 5.0 m was calculated for the event on 05/25/2003 (Event 10) and is illustrated in [Fig. 6](#). On examining

the figure, it is apparent that the resort has a large portion of its territory exposed to the water, with flooding reaching the second through the fifth home court. In the southern sector, a level rise of 5 m climbs the preserved dunes but not completely, with the top of the dunes remaining dry. Thus, even in the face of a very high rise in level, the dunes still retain their role as a natural barrier that protects against advances from the sea. To the Rio Grande do Sul coast, [Guimarães et al. \(2015\)](#) also identified through numerical models the important role of the dunes to the coastal protection, preventing water intrusion on the continent. In the [Fig. 6](#), the two great depressions in the land north and south of the access road to the resort are clear, and the worst-hit areas are precisely those located in the vicinity of inlets, as these regions have lower quotas and are also characterized as access roads for the intrusion of sea water on to the continent.

Due to the higher wind velocity recorded during all the events,

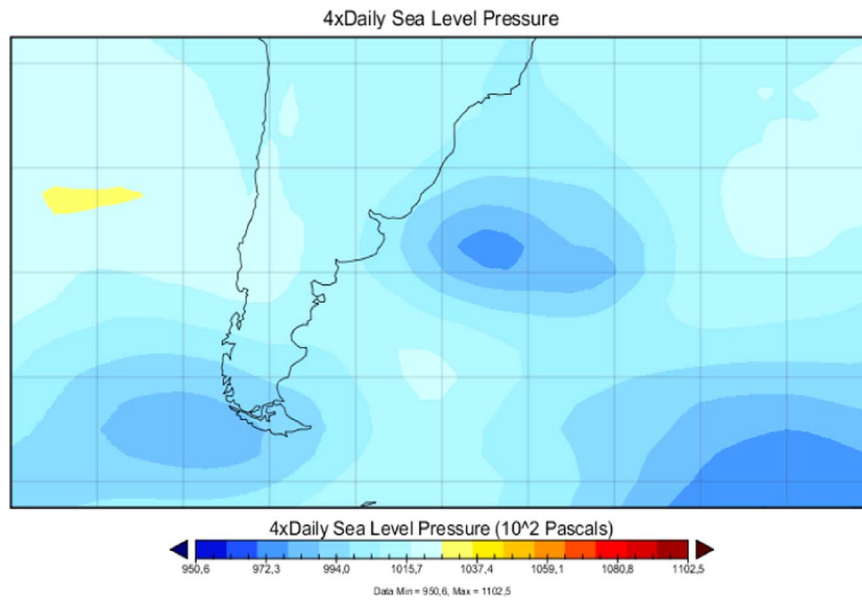


Fig. 9. Low pressure center in the Atlantic Ocean indicating the cyclone during event 10.

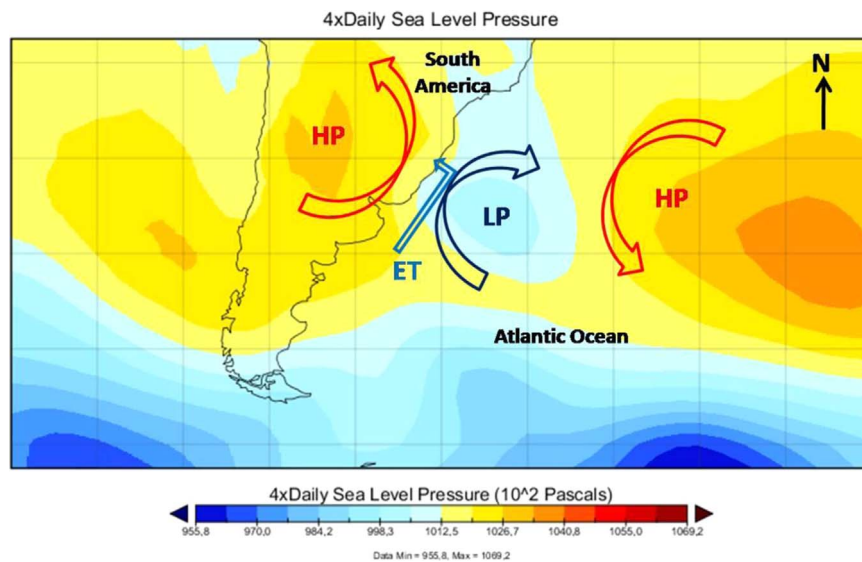


Fig. 10. Stagnant cyclone between two high pressure centers in April 1999.

with 14.9 m/s recorded, as well as the long event duration (66 h), the wind contribution to raising the level was 66%. Thus, due to this high value, the other forcing factors present relatively minor percentage value contributions, with waves contributing 18%, the astronomical tide contributing 10%, and the pressure contributing 5%; these values do not necessarily mean that they have contributed little because the significant wave height was relatively high, 3.6 m, and 8.4 s for the period (Figs. 7 and 8), and the pressure introduced the 3rd largest value variation among other events, with oscillations of 23.3 hPa (Fig. 9). Thus, as in event 14, the high values in wind, wave and pressure properties were responsible for the high value in the elevation level of 5 m, especially the wind.

Calliari and Faria (2003) also studied the event that occurred in May 2003. According to the authors, this event could be observed in the Argentine, Uruguayan and Brazilian coast. Also according to these authors, significant wave heights up to 6.9 m with periods of

up to 12.2 s were recorded by a Brazilian Navy buoy anchored 70 m deep approximately 75 nautical miles SE of Rio Grande.

### 3.5. Positive storm surges and their impact on the Brazilian southern coast

During the events studied, the most important factor for the existence of positive storm surges was the presence of a low pressure center (cyclone) in the Atlantic Ocean over the continental shelf. Off the Brazilian southern coast, cyclones move towards the coast and can stay in this region for hours to days, creating waves and high intensity winds on the Rio Grande do Sul coast. Thus, in these situations, the main cause of storm surges is the continued presence of cyclones coming toward the mainland, which then generate strong winds, high waves, water accumulation and stacking on the coast. According to Tozzi (1999), the location of the center of high pressure is also of great meteorological

importance because this factor may divert the trajectory of cyclones and even make them stagnate in a given area when acting as an atmospheric blocking event. This situation was observed in the April 1999 event (Event 4), in which the cyclone over the continental shelf found itself trapped between two anti-cyclones, one in the middle of the Atlantic Ocean and one on the main land, as shown in Fig. 10. We setup an atmospheric blocking mode to stagnate and prevent the dissipation of the cyclone, which then remained for 102 h over the continental shelf adjacent to the Rio Grande do Sul. According to Machado and Calliari (2016), in a study of 93 extreme events occurring between 1948 and 2013 with NCEP/NCAR reanalysis dataset, the path of the cyclone formed a loop without much forward motion, and this extratropical cyclone presented the lowest propagation velocity of all cyclones studied during this 66 years.

Among all the events analyzed this event was that presented the longer duration time (102 h), almost double that the second (66 h). Thus, because of his long permanence on the platform, and as described above, this event was responsible for the destruction of 20% of sea side houses located in Hermenegildo Beach and numerous others structural damage. According to Machado and Calliari (op cit.) this storm caused severe erosion at this beach,  $45 \text{ m}^3 \text{ m}^{-1}$ . Studying the occurrence of extreme events in southern Brazil, Guimarães et al. (2014) identified an important relationship between geomorphology and waves during storms surges. According to the authors, the wave energy tends to be concentrated in areas of higher gradients of bathymetry and with heterogeneous bottom morphology, as in the Hermenegildo Beach and, although the erosion at this beach has mainly been a problem of anthropic occupation, this relationship between waves and geomorphology shows that this problem can also be associated with the cyclogenesis pattern and the wave transformation at the shoreface, where the waves energy has been concentrated in front of Hermenegildo Beach.

Tozzi (1999) and Parise (2007) consider that cyclones very near the coast have a severe recurring impact, but storms located in the middle of the ocean generate comparatively smaller impacts that are distributed along the coast. Among the events analyzed in this work, one that has more information about the damages, and also considered in the existing literature the most harmful, the April 1999 event (Event 4) has, according to Tozzi and Calliari (2000), an annual return period. Sallenger (2000) proposed a scale of storm impacts in coastal areas, where the most extreme levels, Overwash Regime and Inundation Regime, were observed during the event 10 with sea level rising at 5 m (Fig. 6). At this level, in the areas with sand dunes preserved, is possible to observe both overwash of some sections of the frontal dunes as the transposition of the same and subsequent flooding of the rear area of the dune system. However, even with such increased level of 5 m and the occurrence of both impacts, we can still observe the top of the dune system emerged. So in 400 m of a beach stretch, depending on the morphological variation of sand dunes, it was possible to observe different levels of impact for the same event.

In a sea level lifting scenario, per share of storms, a factor that draws attention when analyzing the illustrations relating to vulnerability to flooding is the presence of inlets. According to Figueiredo and Calliari (2005), these features are quite common in the Rio Grande do Sul coast, where these small-scale water ways play an important role in the drainage of the coastal zone and especially in sediment remobilization of the dune and swash regions. Thus, their presence on the coast is extremely important to the dynamic sand configuration of the frontal dunes. In particular, Hermenegildo Beach has a greater than average concentration of inlets per kilometer of beach compared with the rest of the Rio Grande do Sul coast (Tozzi et al., 1999), with 3 large inlets observed throughout the resort, which extend less than 3 km (Fig. 6).

These structures are interruptions of the dunes and are true weakness zones to the onslaught of the sea. In addition to interrupting the continuity of the dunes, they are areas of low altitude, thereby enhancing the effects of sea level highs on the inlets. This is quite explicit in the illustrations relating to the sea level rise in 5.0 m, where the areas of greatest seawater intrusion are just over the inlets (Fig. 6). To the Rio Grande do Sul coast, Guimarães et al. (2015) also confirmed that the urban occupation in inlets produced a large susceptibility of flooding risk due to water level variations. Another important factor in this context is that in storm situations, the inlets support faster water movement due to the increase in rain fall rates, draining water from the coastal area adjacent to the region. However, with a rising sea level on the coast, this rain water cannot drain and empty into the sea but rather is dammed in the continent, transposing the margins of the inlet sand flooding the region. As the volume of water handled by an inlet is variable, its position and mouth are also dynamic and meander, assuming different degrees of compliance. This feature makes the areas surrounding these inlets more vulnerable and susceptible to marine action, constantly changing the morphology of the dunes. Thus, the flood potential is intensified in areas where the lateral migration of inlets changes the setting of the dunes (Benavente et al., 2006). Inlets of Hermenegildo Beach does not contain containment structures, which allows the horizontal displacement of the shoreline in these areas into the continental interior. Thus, the natural occurrence and patterns of changes produced by urbanization highlight inlets coastal risk characteristics (Figueiredo and Calliari, 2005).

#### 4. Conclusions

An analytical model was developed to calculate sea level rise during storms with satisfactory results. For the study area, the model can be used for reconstitution and forecasting rises in sea level on the coast due to the passage of cyclones.

In the case of the Rio Grande do Sul southern coast during cyclone-induced storms, rising sea levels were forced primarily by the wind (contribution 43%), secondarily by swell (contribution 35%), followed by astronomical tide (contribution 15%) and finally by atmospheric pressure (contribution 7%). Combining the results obtained by applying the analytical model for sea level rises during storms with Digital Terrain Models (DTM) allowed an approximation of the potential flooding of the beach, dune field and adjacent regions, supplementing forecasts and decision making by managers. Such tools are used to support the analysis of coastal risk, although other factors such as the presence of containment structures (walls, spits, etc.) should also be considered in quantifying the degree of risk.

For the Hermenegildo Beach, the following can also be concluded:

The central sector is the most vulnerable to flooding because this segment has less beach width due to sea advancement and restriction of the shoreline by high concentrations of houses on the escarpment. The southern sector of Hermenegildo Beach is the least vulnerable stretch. In this area, urbanization still has a small presence, and the dunes are preserved. This stretch also includes the widest beach, which dissipates wave energy, reducing the impact on this coastal sector. As this section is still preserved, it has greater adaptive capacity for dynamic beach balance, and the dunes are shown to be very efficient structures in terms of natural coastal protection. On the other hand, zones adjacent to the inlets may be considered highly vulnerable to floods.

## Acknowledgements

We gratefully acknowledge CAPES for the financial support offered during this work.

## Appendix

$$\eta t = \eta v + \eta w + \eta p + \eta a.$$

**Equation 1.** Analytical model to calculate the rise in sea level during storms induced by cyclones. Where,

$\eta t$  = total level rise.

$\eta v$  = level rise induced by wind (wind set-up).

$\eta w$  = level rise induced by wave (wave run-up).

$\eta p$  = level rise induced by pressure (barometric set-up).

$\eta a$  = level rise induced by astronomical tide.

$$\eta v = \frac{u_*^2}{f c} [(ft) e^{-\frac{x}{R}}]$$

**Equation 2.** Wind-induced level elevation. Where,

$\eta v$  = level rise induced by wind (wind set-up) (m).

$u_*$  = wind stress on the water surface (m/s).

$f$  = Coriolis parameter (1/s).

$c$  = wave velocity in shallow water (m/s).

$t$  = event duration (s).

$x$  = distance from the point of desired elevation to the coast, adopted here as 0 m (for wanting to achieve a level rise on the coast).

$R$  = Rossby ray strain (m).

Where,

$$f = 2\Omega \sin(\alpha)$$

**Equation 3.** Coriolis parameter.

$$c = \sqrt{gH}$$

**Equation 4.** Wave propagation speed calculation in shallow water.

$$R = \frac{c}{f}$$

**Equation 5.** Rossby ray strain. Where,

$$\Omega = 7.292 \times 10^{-5}.$$

$$\alpha = -34^\circ.$$

$$g = 9.8 \text{ m/s}.$$

$H$  = Average depth of the platform, adopted in this work as 100 m.

And also,

$$u_*^2 = \frac{\tau}{\rho_a}$$

**Equation 6.** Wind surface tension on water.

Where,

$\rho_a$  = water density (1024 kg/m<sup>3</sup>).

$\tau$  = wind shear stress.

$$\tau = \rho_{ar} C_d V^2$$

**Equation 7.** Wind shear stress. Where,

$\rho_{ar}$  = air density (1.25 kg/m<sup>3</sup>).

$V$  = wind speed parallel to the coast (m/s).

$C_d$  = wind drag coefficient, which is dependent on the wind speed and is derived from Bowden (1983).

$$\eta o = (H_s L_0')^{0.5} \tan \beta$$

**Equation 8.** Wave run-up. Where,

$H_s$  = significant wave height in deepwater.

$L_0$  = wave length.

$\beta$  = slope from the beach face in degrees, adopted here as 2.6°, taken from Pereira et al. (2010).

And also,

$$L_0' = 1.56 T^2$$

**Equation 9.** Wave length. Where,

$T$  = peak period associated with the significant wave height.

$$\eta p = \frac{\Delta P}{\rho_a g}$$

**Equation 10.** Pressure-induced level elevation by Inverse Barometer Effect. Where,

$\eta p$  = level rise induced by pressure (barometric set-up).

$\Delta P$  = atmospheric pressure variation (Pa).

$\rho_a$  = water density (1024 kg/m<sup>3</sup>).

$g$  = 9.8 m/s.

$$Y = 0.817x + 0.2252$$

**Equation 11.** Equation from linear correlation between sea level elevation values measured in the field (Parise et al., 2009) and calculated by the analytical model.

## References

- Balsillie, J.H., 1986. Beach and coast erosion due to extreme event impact. *Shore and Beach* 54 (4), 22–37.
- Battjes, J., 1971. Run-up distributions of waves breaking on slopes. *J. Waterw., Harb. Coast. Eng. Div.* 97, 91–114.
- Benavente, J., Garcia, F.J., López-Aguayo, F., 2000. Empirical model of morphodynamic beachface behaviour for low-energy mesotidal environments. *Mar. Geol.* 167, pg375–390.
- Benavente, J., Del Río, L., Anfuso, G., Gracia, F.J. e Reyes, J.L., 2002. Utility of Morphodynamic Characterisation in the Prediction of Beach Damage by Storms. *J. Coast. Res. SI 36 56–64* (ICS 2002 Proceedings) Northern Ireland ISSN 0749–0208.
- Benavente, J., Del Río, L., Gracia, F.J., Martínez-del-Pozo, J.A., 2006. Coastal flooding hazard related to storms and coastal evolution in Valdelagrana spit (Cadiz Bay Natural Park, SW Spain). *Cont. Shelf Res.* 26 (2006), 1061–1076.
- Bowden, K.F., 1983. *Physical Oceanography of Coastal Waters*. Ellis Horwood Ltd., Chichester England, p. 301.
- Callaghan, D.P., Ranasinghe, R., e Short, A., 2009. Quantifying the storm erosion hazard for coastal planning. *Coast. Eng.* 56, 90–93.
- Calliari L.J., Faria, A.F.G., 2003. Bancos De Lama na Praia Do Cassino: Formação, Implicações geomorfológicas, ambientais e riscos costeiros, estudo De caso: maio De 2003. *Anais Do IX Congresso da Associação Brasileira De Estudos Do Quaternário*.
- CEPAL-ONU –Efectos Del cambio climático En La Costa De América Latina y EL Caribe, 2011.
- Csanady, G.T., 1982. *Circulation in the Coastal Ocean*. D.Reidel Publishing Company, Dordrecht, Holland/Boston, U.S.A/London, England, 279 p.
- Esteves, L.S., Vranjac. M.P., Barletta, R.C., Pivel, M.A.G., Erthal, S., Vanz, A., Silva, A.R. P., Oliveira, U.R., 1999. Impacto de um evento de alta energia nas obras de proteção costeira no balneário do Hermenegildo, RS, Brasil. *Anais Do VII Congresso da ABEQUA, Porto Seguro – BA*.
- Esteves, L.S., Pivel, M.A.G., Silva, B., Vranjac, M.P., Oliveira, U.R., R.C., A.R.P., Vanz, A., 2000. Beach owners perception of beach erosion along na armored shoreline in southern Brasil. *Pesqui. Em Geociênc.* 27 (2), 93–109.
- Ferreira, O., Garcia, T., Matias, A., Taborda, R., Alveirinho, J.D., 2006. An integrated method for the determination of set-back lines for coastal erosion hazards on sandy shores. *Cont. Shelf Res.* 26, 1030–1044.
- Figueiredo, S.A., Calliari, L.J., 2005. Sangradouros: Distribuição Espacial, Variação Sazonal, Padrões Morfológicos e Implicações no Gerenciamento Costeiro. *GRAVEL, Porto Alegre, ISSN 1678–5975, no. 3, pp. 47–57*.
- Freitas, D., Araújo, R.S., Klein, A.H.F., e Menezes, J.T., 2010. Quantificação dos perigos costeiros e projeção de linhas de costa futuras para a enseada de Itapocoróí – SC. *Braz. J. Aquat. Sci. Technol.* 14 (1), 39–49.
- Gill, A.E., 1982. *Atmosphere-Ocean Dynamics*. Academic Press, New York, p. 662.
- Goring, D.E., 1995. Short-term variations in sea level (2–15 days) in the New Zealand region. *N.Z. J. Mar. Freshw. Res.*, 1995 29, 69–82.
- Goulart, E.S., 2010. Morfodinâmica da antepraia adjacente ao Farol da Conceição: litoral médio do RS. *Dissertação de mestrado, Universidade Federal do Rio Grande, Furg*.
- Guimarães, P.V., Farina, L., Toldo Jr, E., 2014. Analysis of extreme wave events on the southern coast of Brazil. *Nat. Hazards Earth Syst. Sci.* 14, 3195–3205.
- Guimarães, P.V., Farina, L., Toldo Jr, E., Diaz-Hernandes, G., Akhmatkaya, E., 2015.

- Numerical simulation of extreme wave runup during storm events in Tramandai Beach, Rio Grande do Sul, Brazil. *Coast. Eng.* 95, 171–180.
- Lawrence, P.L., 1994. Natural hazards of shoreline bluff erosion: a case study of Horizon View, Lake Huron. In: Morisawa, M. (Ed.), *Geomorphology and Natural Hazards* vol. 10. Geomorphology, pp. 65–81.
- Machado, A.A., Calliari, L.J., 2016. Synoptic systems generators of extremes wind in southern Brazil: atmospheric conditions and consequences in the coastal zone. Proceedings of the 14th International Coastal Symposium, Sydney, Australia. *J. Coast. Res.*, Special Issue, No. 75, pp. 1182–1186. Coconut Creek, Florida, ISSN 0749–0208.
- Machado, A.A., Calliari, L.J., Melo, E., e Klein, A.H.F., 2010. Historical assessment of extreme coastal sea state conditions in southern Brazil and their relation to erosion episodes. *Pan-Am. J. Aquat. Sci.* 5 (2), 277–286.
- Maia, N.Z., 2011. Avaliação da elevação do nível do mar e riscos de inundação costeira associados à passagem de ciclones no balneário Hermenegildo, RS. Dissertação de mestrado. Universidade Federal do Rio Grande, FURG. 118 p.
- Marone, E. e, Camargo, R., 1994. Marés Meteorológicas no estado do Paraná: o evento de 18 de agosto de 1993. *Nerítica, Curitiba* 8 (1–2), 55–72 (Editora da UFPR).
- Melo, E., Romeu, M.A.R., Hammes, G.R., 2010. Condições extremas de agitação marítima ao largo de Rio Grande a partir do Modelo WW3. IV Seminário e Workshop em Engenharia Oceânica – FURG(SEMENGO), Rio Grande do Sul, Brasil, 20 p.
- Morton, R.A., Leach, M.P., Paine, J.G., Cardoza, M.A., 1993. Monitoring beach changes using GPS surveying techniques. *J. Coast. Res.* 9 (3), 884–908.
- Morton, R.A., Speed, F.M., 1998. Evaluation of shorelines and legal boundaries controlled by water levels on sandy beaches. *J. Coast. Res.* 14 (4), 1373–1384.
- Oliveira, M.M.F., Ebecken, N.F.F., Santos, I.A., Neves, C.F., Caloba, L.P., Oliveira, J.L.F., 2007. Modelagem da maré meteorológica utilizando redes neurais artificiais: uma aplicação para a baía de Paranaguá – PR, parte 2: dados meteorológicos de REANÁLISE do NCEP/NCAR. *Rev. Bras. De Meteorol.* 22 (1), 53–62.
- Pajak, M.J., Leatherman, S., 2002. The high water line as shoreline indicator. *J. Coast. Res.* 18 (2), 329–337.
- Parise, C.K., 2007. Padrões atmosféricos sinóticos geradores de mares meteorológicas intensas e a resposta morfodinâmica da praia do Cassino. Trabalho De conclusão De curso De Oceanologia. Universidade Federal Do Rio Grande, FURG.
- Parise, C.K., Calliari, L.J., Krusche, N., 2009. Extreme storm surges in the south of Brazil: atmospheric conditions and shore erosion. *Braz. J. Ocean.* 57 (3), 175–188.
- Pereira, P.S., Calliari, L.J., Barletta, R.C., 2010. Heterogeneity and homogeneity of Southern Brazilian beaches: a morphodynamic and statistical approach. *Cont. Shelf Res.* 30, 270–280.
- Pugh, D.T., 1987. *Tides, Surges and Mean Sea Level. A Handbook for Engineers and Scientists.* John Wiley&Sons Ltd., New York, p. 472.
- Santos, I.R., e Esteves, L.S., 2001. Evolução das obras de proteção costeira no Hermenegildo (RS) entre 1999–2001. Anais da XIV Semana Nacional de Oceanografia. Rio Grande, RS, Brasil.
- Sallenger, A.H., Jr. 2000. Storm Impact Scale for Barrier Island. *J. Coast. Res.*, vol. 16 (3), pp. 890–895. West Palm Beach, Florida, ISSN 0749–0208.
- Saraiva, J.M.B., Bedran, C. e, Carneiro, C., 2003. Monitoring of storm surges on Cassino Beach. *J. Coast. Res. Spec. Issue* 35, 323–331.
- Tagliani, C.R., Calliari, L.J., Tagliani, P., e Antiquiera, J.A., 2010. Vulnerability to sea level rise of an estuarine island in southern Brazil. *Quat. Environ. Geosci.* 01 (1), 18–24.
- Teixeira, P.S., 2007. Subsídios Para o gerenciamento costeiro por erosão da falésia No balneário Hermenegildo. Dissertação apresentada como requisito parcial à obtenção Do grau De Mestre Em Oceanografia Física, Química e Geológica. Universidade Federal Do Rio Grande, FURG.
- Toldo Jr, E.E., Almeida, L.E.S.B., Martins, L.R.S., Gruber, N.L.S., Barros, C.E., Nicolodi, J. L., Farina, L. e Nunes, J.C., 2010. Hidrodinâmica e Sedimentologia das Praias Oceânicas do Rio Grande do Sul. Instituto de Geociências. Contribuições. 50 anos de Geologia. Universidade Federal do Rio Grande do Sul.
- Tolman, H.L., 1997. User manual and system documentation of WAVEWATCH- III version 1.15 NOAA/NWS/NCEP/OMB Technical Note, 151, 97 pp.
- Tolman, H.L., 2002. User manual and system documentation of WAVE-WATCH III version 2.22. NOAA/NWS/NCEP/OMB Technical Note 222, 130 pp.
- Tozzi, H.A.M., 1999. Influência das tempestades extratropicais sobre o estoque subaéreo das praias entre Rio Grande e Chuí, RS. Campanha do outono e inverno de 1996. Dissertação De mestrado. Universidade Federal Do Rio Grande, FURG.
- Tozzi, H.A.M., e Calliari, L.J., 2000. Morfodinâmica da Praia do Cassino, RS. *Pesqui. Em Geociênc.* 27 (1), 29–42.
- Tozzi, H.A.M., Pereira da Silva, R., Calliari, L.J. e Barletta, R.C., 1999. Variações de curto e longo período na morfologia das praias entre Cassino e Hermenegildo, Rio Grande do Sul. Anais Do VII Congresso da ABEQUA, Porto Seguro – BA.
- Truccolo, E.C., Franco, D., e Schettini, C.A.F., 2006. The Low Frequency Sea Level Oscillations in the Northern Coast of Santa Catarina, Brazil. *J. Coast. Res.* SI 39, 547–552 ICS 2004 (Proceedings) Brazil ISSN 0749–0208.
- Van Cooten, S., Kelleher, K.E., Howard, K., Zhang, J., Gourley, J.J., Kain, J.S., Nemunaitis-Monroe, K., Flamig, Z., Moser, H., Arthur, A., Langston, C., Kolar, R., Hong, Y., Dresback, K., Tromble, E., Vergara, H., Luettich Jr., R.A., Blanton, B., Lander, H., Galluppi, K., Losego, J.P., Blain, C.A., Thigpen, J., Mosher, K., Figurskey, D., Moneyppenny, M., Blaes, J., Orrock, J., Bandy, R., Goodall, C., Kelley, J.G.W., Greenlaw, J., Wengren, M., Eslinger, D., Payne, J., Olmi, G., Feldt, J., Schmidt, J., Hamill, T., Bacon, R., Stickney, R., Spence, L., 2011. The CI-FLOW project: a system for total water level prediction from the summit to the sea. *Bull. Am. Meteorol. Soc.* 92, 1427–1442.
- Van Rijn, L.C., 2009. Prediction of dune erosion due to storms. *Coast. Eng.* 56 (2009), 441–457.
- Xavier, A.L.M., 2003. Influência do padrão atmosférico nas marés meteorológicas na Praia do Cassino, Rio Grande, RS. Trabalho De conclusão De curso De Oceanologia. Universidade Federal Do Rio Grande, FURG.
- (<http://www.cpc.ncep.noaa.gov/products/wesley/reanalysis.html#intro>) (accessed 26.03.16).
- (<http://www.esrl.noaa.gov/psd/data/gridded/reanalysis/>) (accessed 26.03.16).